

# UniASM: Binary Code Similarity Detection without Fine-tuning

Yeming Gu<sup>1</sup>, Hui Shu<sup>1,\*</sup> and Fan Hu<sup>1</sup>

<sup>1</sup> State Key Laboratory of Mathematical Engineering and Advanced Computing, Zhengzhou, 450000, China

**Abstract:** Binary code similarity detection (BCSD) is widely used in various binary analysis tasks such as vulnerability search, malware detection, clone detection, and patch analysis. Recent studies have shown that the learning-based binary code embedding models perform better than the traditional feature-based approaches. In this paper, we propose a novel transformer-based binary code embedding model named UniASM to learn representations of the binary functions. We design two new training tasks to make the spatial distribution of the generated vectors more uniform, which can be used directly in BCSD without any fine-tuning. In addition, we present a new tokenization approach for binary functions, which increases the token’s semantic information and mitigates the out-of-vocabulary (OOV) problem. We conduct an in-depth analysis of the factors affecting model performance through ablation experiments and obtain some new and valuable findings. The experimental results show that UniASM outperforms the state-of-the-art (SOTA) approach on the evaluation dataset. The average scores of Recall@1 on cross-compilers, cross-optimization levels, and cross-obfuscations are 0.77, 0.72, and 0.72. Besides, in the real-world task of known vulnerability search, UniASM outperforms all the current baselines.

**Keywords:** Similarity Detection; Embedding; Binary Code; Assembly Language; Vulnerability

## 1 Introduction

Binary code similarity detection (BCSD) is widely used in vulnerability search [1, 2], malware detection [3-5], clone detection [6, 7], patch analysis [8], etc. Most commercial software is closed-sourced and consists of a large amount of binary code. Therefore, the study of BCSD has crucial practical significance.

One of the main challenges of BCSD is that different compilers, optimization levels, or code obfuscations can lead to significant changes in the binary code. The target binaries lose most of the natural semantic information of the source code during the compilation process. Since the binary code does not have vocabularies containing natural semantics as the source code, extracting semantic features from it is challenging. Sæbjørns et al. [9] try to extract statistical features of instructions for BCSD manually. However, the statistical characteristics vary with the compilation optimization options, resulting in a degradation of BCSD performance. Other works [10, 11] try to analyze similarity through the control flow graph (CFG). However, different compile options or code obfuscations may lead to different CFGs.

As none of the traditional similarity comparison methods have addressed the problem of cross-optimization levels and cross-obfuscations, the deep learning-based models are considered promising candidate methods for BCSD. In recent years, natural language processing (NLP) models have shown their capabilities of semantic understanding and text embedding. The state-of-the-art research in BCSD has begun to employ NLP models. Asm2vec [12] generates embeddings for instructions and functions based on the PV-DM model [13]. SAFE [14] uses the skip-gram method [15] and self-attention network [16] to generate the embedding. However, neither PV-DM nor skip-gram can learn the complex semantic features of the binary code because they rely heavily on instructions of similarity in the binary code pairs. Recent studies try to use more complex models: PalmTree [17] is the first to apply BERT [18] to instruction embedding, and jTrans [19] leverages BERT to learn the

control flow information of the functions. They achieved better performance than traditional methods. However, some key issues need to be studied in depth:

- Which backbone model should be chosen for binary code embedding?
- What training tasks are better for BCSD?
- How to serialize the assembly code properly?

This paper proposes a toolkit called UniASM, designed to achieve high BCSD performance and can be used directly without fine-tuning. We have created two training tasks for UniASM: Assembly Language Generation (ALG, Section 3.4.1) and Similar Function Prediction (SFP, Section 3.4.2). ALG predicts the second function in the input sequence based on unidirectional attention, while SFP predicts the similarity of the two functions in the input sequence. After training, the generated function embeddings can be used for BCSD tasks directly.

The contributions of this paper are summarized as follows:

(1) We propose a novel assembly language processing model, UniASM, the first UniLM-based model for BCSD. Our model outperforms the baselines and can be used in the real-world vulnerability search task. We have released the code and the pre-trained model of UniASM at <https://github.com/clm07/UniASM>.

(2) We propose a new representation approach for binary functions (Section 3.2), which uses well-designed normalization of instructions to make a balance between out-of-vocabulary (OOV) and semantic learning.

(3) We design ablation studies to explore the impact of different backbone models, training tasks, serialization methods, tokenization algorithms, and sequence lengths on the model’s accuracy in BCSD tasks. Some new findings ignored by existing studies are found:

- Even without training, the UniLM-based model achieves considerable performance in BCSD tasks and is significantly better than the BERT-based model (Section 5.2.1).
- The pre-training task ALG is more suitable for BCSD than the widely used MLM (Section 5.2.2).
- Neither random-walk nor longest-walk performs any better than the linear serialization of a function (Section 5.2.3).
- Full-instruction tokenization shows better performance than fine-grained algorithms (Section 5.2.4).
- Transformer-based function similarity analysis does not require a very long input sequence length. A fixed length of 256 is sufficient for achieving good performance (Section 5.2.5).

## 2 Related Works

### 2.1 Traditional BCSD Approaches

BCSD is one of the popular research areas of binary analysis. Earlier studies tend to implement vectorization of binary codes by extracting dynamic or static features.

**Dynamic approaches.** Dynamic methods collect run-time information by executing the program in reality or simulation. BinHunt [20] and iBinHunt [21] extract the semantics of functions through symbolic execution and deep taint analysis. However, symbolic execution incurs high costs and is difficult to run on large-scale binaries. The basic idea of Blex [22], BinGo [23], BinGo-E [24], and Multi-MH [25] is to obtain the I/O values of functions by executing the target program. The main shortcoming of these dynamic methods is that the I/O values cannot fully represent the semantics of the function. CACompare [6] and BinMatch [26] leverage emulate executions to obtain richer function semantics to improve similarity comparison performance. IMF-sim [27] and BinSim [28] use finer-grained run-time features to identify differences between two execution traces.

Dynamic approaches can obtain additional run-time features, such as parameters, I/O values, and execution traces. However, they are computationally expensive and require a complex analysis environment, which limits practical usage.

**Static approaches.** Static features such as instructions, basic blocks, function calls, and control flow are used to achieve similarity comparison. IDA FLIRT [29] and UNSTRIP [30] identify library functions by generating fingerprints statically. BinClone [31], ILINE [32], MutantX-S [33], BinSign [34], and BinShape [35] use statistical features of binary code to achieve similarity analysis. Tracelet [36] and BinSequence [37] focus on instruction sequences and use edit distance to compare two instruction sequences. ESH combines the similarity of code fragments to ultimately measure the similarity between procedures. In order to better utilize the control flow information of functions, TEDEM [38], XMATCH [39], and Sæbjørns et al. [9] use tree edit distance or graph edit distance to compare the CFGs of functions. However, comparison based on edit distance is computationally complex and sensitive to structural changes. To address this, DiscovRe [40], BinDiff [41], Genius [42], and Kam1n0 [7] leverage graph isomorphism instead of comparing edit distance to improve the efficiency of graph comparison. The disadvantage of graph isomorphism is that it requires high-quality node features.

## 2.2 Learning-based BCSD Approaches

Deep learning has achieved satisfactory results in tasks such as image processing and language understanding. Recent studies have started to apply learning-based methods to BCSD tasks.

**DNN-based approaches.** Deep Neural Network (DNN) is a multi-layer neural network mainly used to process images, audio, and text. Inspired by image processing, Marastoni et al. [43] translated binaries into images and used Convolutional Neural Networks (CNN) to process the generated images, achieving program classification. However, this method can only be applied to small binaries because the CNN network needs to see the entire binary image.  $\alpha$ diff [1] works on the function instead of the whole binary and learns function embeddings directly from the sequence of raw bytes using CNN. VulSeeker [44] extracts basic block features and inputs them into a DNN to generate function embeddings for vulnerability function search. DNN-based methods cannot handle the order information of input data well, while the execution order is crucial to the code semantics.

**Graph-based approaches.** Graph Neural Network (GNN) can directly process graph data and can be used to learn program semantics from control flow, data flow, and function call relationships. Gemini [11] and GraphEmb [45] extract attributed control flow graphs (ACFGs) for functions and train a graph embedding network to generate embeddings. GMNN [46] proposes graph matching networks to generate similarity scores instead of generating embeddings separately to compute the similarity between graphs more efficiently. BugGraph [10] utilizes a graph triplet-loss network on the ACFG to produce a similarity ranking. Bin2vec [47] attempts to use graph convolutional networks to improve the processing performance of graph embeddings. HBinSim [48] believes that different features of functions should have different weights in BCSD, so it uses a hierarchical attention graph embedding network to implement ACFG embedding. Asteria [49] extracts the syntax tree of functions instead of CFG and uses a Tree-LSTM network to generate function embeddings. However, both graph embeddings and Tree-LSTM face the problem of high computational complexity for large-scale graph data and heavily rely on the accuracy of node features.

**NLP-based approaches.** Natural Language Processing (NLP) has shown excellent performance in text processing and semantic understanding tasks. It can also be used for semantic learning from binary code by extracting assembly semantics. Asm2vec [12] generates embeddings for instructions and functions using the word2vec model [50]. In addition to word2vec, InnerEye [2] utilizes Long Short-Term Memory (LSTM) to

learn basic block embeddings. Zhengping Luo et al.’s research [51] uses a Siamese network to implement similarity comparison of basic block embeddings generated by LSTM. To learn more semantics, Transformer-based models have become a research hotspot in recent years. PalmTree [17], DeepSemantic [52], and BinShot [53] apply the BERT model [18] to binary code embedding and show the great potential of language models in BCSD. MIRROR [54] aims to cross-architecture similarity analysis by a transformer-based neural machine translation model. Transformer-based approaches require translating instructions or functions into a sequence, which may lead to the loss of function control flow information. To address this, jTrans [19] is the first study to embed control flow information of binary code into Transformer-based language models.

**Hybrid approaches.** As single methods always have limitations, some studies attempt to mix multiple models to achieve better BCSD performance. SAFE [14] uses word2vec to generate instruction embeddings and then utilizes a self-attentive neural network to generate function embeddings. DeepBinDiff [55] first trains a token embedding model derived from word2vec and then leverages the Text-associated DeepWalk [56] algorithm to learn basic block embeddings from the inter-procedural control-flow graphs. BinDNN [57] utilizes three types of neural network models: CNN, LSTM, and regular fully connected feed-forward neural networks. There are other hybrid approaches, such as BEDetector [58], which combines NLP model and graph auto-encoder model to generate function embeddings, and Codee [59], which combines NLP model and network representation learning model. OrderMatters [60] integrates more models, including word2vec, BERT, MPNN [61], and CNN. Although hybrid methods can achieve complementary advantages, they make model training and usage more difficult, and data processing and computational costs are relatively high.

Overall, Learning-based BCSD methods have better adaptability and performance than traditional methods. Among them, Transformer-based methods show the best potential performance. However, existing researches have only tried BERT-based methods, and research on model training and data processing is still insufficient. Further research is needed, including backbone models, training tasks, tokenization methods, etc.

## 3 Methodology

### 3.1 Overview

UniASM is mainly inspired by SimBERT [62] and UniLM [63]. UniLM uses bidirectional and unidirectional attention to achieve semantic understanding and generative capabilities. SimBERT proposes a new similarity query task for each batch. UniASM is a transformer-based model and uses two training tasks: Assembly Language Generation (ALG) and Similar Function Prediction (SFP). ALG leverages unidirectional attention to generate the second half of the sequence. SFP is a function query task similar to the query task in SimBERT, which enables the generated function embeddings to be used directly in the BCSD tasks.

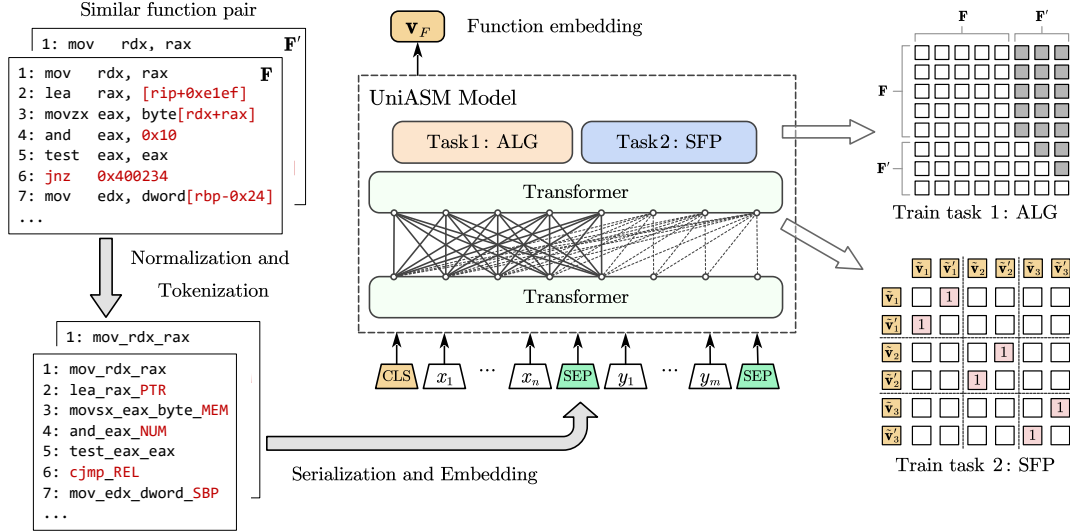


**Figure 1:** Overview of UniASM

Figure 1 shows an overview of UniASM. For training, the input sequence is constructed from a pair of similar functions. First, the instructions of the functions are normalized to remove the noisy words and mitigate the OOV problem. Then, the instructions are tokenized according to a simple principle: one instruction produces one token. Next, we use a simple linear serialization approach to convert a function into a sequence of tokens. Finally, the sequence is used as the input of UniASM.

For evaluation, the input sequence is constructed from one function, and the output of the model is the function embedding. We compute the cosine similarity between the two function embeddings as our model-predicted similarity.

### 3.2 Function representation

The raw representation of a binary function is a series of instructions that cannot be used directly. We design a new representation approach for binary functions. It mainly contains three stages: instruction normalization, assembly tokenization, and function serialization.

#### 3.2.1 Instruction Normalization

Instruction normalization makes instructions look cleaner by replacing the addresses, immediate numbers, float instructions, and conditional jumps. The main principles are as follows:

- The indirect addressing with register *eip/rip* is replaced by *PTR*
- The indirect addressing with register *esp/rsp* is replaced by *SSP*
- The indirect addressing with register *ebp/rbp* is replaced by *SBP*
- Other indirect addressing is replaced by *MEM*
- The relevant addressing is replaced by *REL*
- The immediate number is replaced by *NUM*
- The float instruction with register *xmm* is replaced by *XMM*
- The conditional jump, such as *jnz*, is replaced by *cjmp*

#### 3.2.2 Assembly Tokenization

Tokenization decomposes unstructured data and texts into chunks of information that can be considered discrete elements called tokens. In this paper, the whole instruction is treated as a token. The advantage is that

the instruction contains richer semantic information than individual operands. In practice, we replace the white space with an underline for an instruction, e.g., “mov rax, 0x10” will be represented by the token “mov\_rax\_NUM.” The ablation study (Section 5.2.4) shows that this full-instruction tokenization approach performs much better than the fine-grained approaches.

### 3.2.3 Function Serialization

Function serialization aims to serialize the structured function into a sequence of tokens. The approach used in this paper is to serialize the function directly in linear order (address order). Experimental results (Section 5.2.3) show that linear serialization performs similarly to random-walk and longest-walk. However, random-walk and longest-walk require the construction of a CFG of the function, which is time-consuming. Even worse, longest-walk has to search the longest path on the CFG, which is difficult.

### 3.3 Backbone network

The base model used in UniASM is a transformer model, as shown in Figure 2, which has shown a strong capability in the representation learning of natural semantics. According to the processing flow, it can be divided into three parts: the token embedding layer, the self-attention layer, and the function embedding layer.

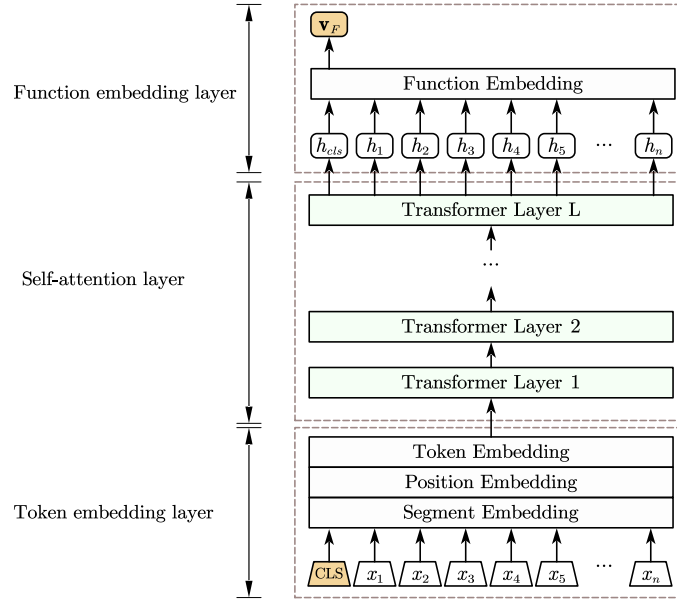


**Figure 2: Backbone network**

#### 3.3.1 Token Embedding Layer

The token embedding layer is used to generate the input vector for the token sequence of the function. For the token sequence of the input function  $\mathbf{F} = [x_1, x_2, \dots, x_n]$ , where  $x_i$  represent the  $i$ -th token of the function, the input vector  $\mathbf{H}^0 = [E(x_1), E(x_2), \dots, E(x_n)]$  is obtained by summing the token embedding  $Ex_i$ , position embedding  $Ep_i$ , and segment embedding  $Es_i$ :

$$E(x_i) = Ex_i + Ep_i + Es_i.$$

#### 3.3.2 Self-attention Layer

The self-attentive layer consists of multiple transformer layers stacked on top of each other, as shown in Figure 2. The input vector  $\mathbf{H}^0 = [E(x_1), E(x_2), \dots, E(x_n)]$  is used as the input to the first layer of the Transformer. For the Transformer with the total number of  $L$  layers, the output of the  $l$ -th layer is represented as  $\mathbf{H}^l = \text{Transformer}_l(\mathbf{H}^{l-1}), l \in [1, L]$ , and the self-attention is calculated as follows:

$$\begin{aligned} \mathbf{Q}_l &= \mathbf{H}^{l-1} \mathbf{W}_l^Q, \mathbf{K}_l = \mathbf{H}^{l-1} \mathbf{W}_l^K, \mathbf{V}_l = \mathbf{H}^{l-1} \mathbf{W}_l^V \\ \mathbf{M}_{ij} &= \begin{cases} 0, & \text{allow to attend} \\ -\infty, & \text{prevent from attending} \end{cases} \\ \mathbf{A}_l &= \text{softmax} \left( \frac{\mathbf{Q}_l \mathbf{K}_l^\top}{\sqrt{d_k}} + \mathbf{M} \right) \mathbf{V}_l \end{aligned}$$

where the output of the previous layer  $\mathbf{H}^{l-1}$  generates  $\mathbf{Q}_l$ ,  $\mathbf{K}_l$  and  $\mathbf{V}_l$  through three parameter matrices  $\mathbf{W}_l^Q$ ,  $\mathbf{W}_l^K$ ,  $\mathbf{W}_l^V$ . The mask matrix  $\mathbf{M}_{ij}$  defines the attention between the tokens. The output  $\mathbf{A}_l$  is summed with the  $\mathbf{H}^{l-1}$  residual operation and the feed-forward network finally generates a new hidden layer vector  $\mathbf{H}^l$ .

### 3.3.3 Function Embedding Layer

The function embedding layer generates the embedding vector of the input function. In this paper, we calculate the function embedding vector by the output vector of the token ‘‘CLS’’:

$$\mathbf{v}_F = \tanh(h_{\text{CLS}}) \cdot \mathbf{W}^F,$$

where  $\tanh(\cdot)$  is the activation function,  $\mathbf{W}^F$  is the parameter matrix of the fully connected network.

## 3.4 Training tasks

UniASM abandons the commonly used mask language model (MLM) and next sentence prediction (NSP) pre-training tasks of BERT in favor of the Assembly Language Generation task (ALG, Section 3.4.1) and the Similar Function Prediction task (SFP, Section 3.4.2).

### 3.4.1 Assembly Language Generation

ALG leverages an attention mask matrix to define bidirectional attention and unidirectional attention. As shown in Figure 3, the first function in the input sequence uses bidirectional attention, while the second function uses unidirectional attention. It allows the model to generate the second function according to the first one.

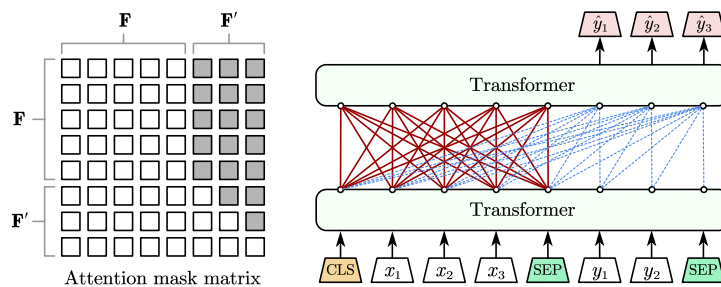


**Figure 3: Assembly Language Generation**

For the input pair of functions  $\mathbf{F}=[x_1, x_2, \dots, x_n]$  and  $\mathbf{F}'=[y_1, y_2, \dots, y_m]$ , the input tokens for UniASM are  $[\text{CLS}, x_1, \dots, x_n, \text{SEP}, y_1, \dots, y_m, \text{SEP}]$ . The goal of ALG is to correctly predict the second function  $\mathbf{F}'$  according to the first function  $\mathbf{F}$ . When we get the predict value  $\hat{\mathbf{F}}'=[\hat{y}_1, \hat{y}_2, \dots, \hat{y}_m]$ , the *softmax* is applied to the result:

$$p(\hat{y}_i | \mathbf{F}) = \frac{\exp(\hat{y}_i)}{\sum_{k=1}^m \exp(\hat{y}_k)},$$

where  $\hat{y}_i$  denotes the predict value of  $y_i$ . ALG uses cross-entropy to calculate the loss as follows:

$$\min_{\theta} \mathcal{L}_{ALG}(\theta) = \sum_i -\log p(\hat{y}_i | \mathbf{F}).$$

### 3.4.2 Similar Function Prediction

SFP processes one batch rather than a pair of functions at a time. As shown in Figure 4, each sample in the batch is a pair of similar functions, such as  $[\text{CLS}] \mathbf{F} [\text{SEP}] \mathbf{F}' [\text{SEP}]$ , where  $\mathbf{F}$  and  $\mathbf{F}'$  are similar functions. We swap these two functions to construct a new sample  $[\text{CLS}] \mathbf{F}' [\text{SEP}] \mathbf{F} [\text{SEP}]$  and place it after the original one. So, each batch should contain an even number of samples.

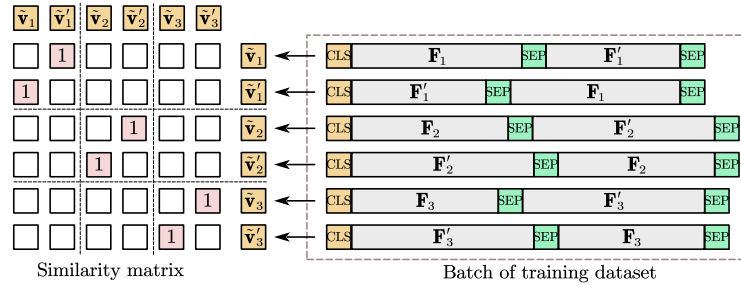


**Figure 4: Similar Function Prediction**

The embedding of the  $k$ -th function in the batch is  $\mathbf{v}_k=[v_1, v_2, \dots, v_d]$ , where  $d$  is the hidden size. Then the elements in the vector are L2 normalized:

$$\tilde{v}_i = \frac{v_i}{\sqrt{\sum_{j=1}^d v_j^2}}.$$

The normalized function embedding vector can be obtained:  $\tilde{\mathbf{v}}_k=[\tilde{v}_1, \tilde{v}_2, \dots, \tilde{v}_d]$ . We take all the normalized vector of the batch to construct the embedding matrix  $\tilde{\mathbf{V}}=[\tilde{\mathbf{v}}_1, \tilde{\mathbf{v}}_2, \dots, \tilde{\mathbf{v}}_b]^\top$ , where  $b$  is the batch size.

To calculate the similarity between two functions in the batch, we dot product the embedding matrix  $\tilde{\mathbf{V}}$  with its transposed matrix  $\tilde{\mathbf{V}}^\top$ :



$$\mathbf{S} = \tilde{\mathbf{V}} \cdot \tilde{\mathbf{V}}^\top = \{s_{ij}\}, i, j \in [1, 2, \dots, b].$$

The result  $\mathbf{S}$  is called the similarity matrix. Each value in the similarity matrix denotes the similarity of two functions. The idea is based on the fact that the value of the dot product of unit vectors is equal to  $\cos(\varphi)$ , where  $\varphi$  denotes the angle between two vectors. The more similar the vectors are, the smaller the angle between them should be. That is, the dot product of vectors of similar functions should be closer to 1, and the dot product of vectors of different functions should be closer to -1.

It should be noted that values on the diagonal in the similarity matrix are all equal to 1 because they are dot products of the same unit vector. However, we only care about the value of the two similar functions. To avoid the effect of the diagonal elements, we set all diagonal elements to negative infinity:

$$\mathbf{S} = \tilde{\mathbf{V}} \cdot \tilde{\mathbf{V}}^\top - \Lambda[+\infty],$$

where  $\Lambda[+\infty]$  denotes a diagonal matrix, whose values are set to infinity. Each row of the matrix needs to be processed by *softmax* layer as:

$$p(s_{ij}) = \frac{\exp(s_{ij})}{\sum_{k=1}^b \exp(s_{ik})},$$

where  $s_{ij}$  denotes the similarity of the  $i$ -th function and the  $j$ -th function in the batch. SFP uses cross-entropy to calculate the loss as follows:

$$\min_{\theta} \mathcal{L}_{SFP}(\theta) = \sum_k -\log p(s_{ik}).$$

The loss function of UniASM is the combination of the two loss functions:

$$\min_{\theta} \mathcal{L}(\theta) = \mathcal{L}_{ALG}(\theta) + \mathcal{L}_{SFP}(\theta).$$

## 4 Experimental setups

### 4.1 Dataset

#### 4.1.1 Training Dataset

As shown in Table 1, we collected seven open-source projects commonly used under Linux as the training dataset for UniASM.

**Table 1:** Projects Used for Training

Projects	Version	Binaries	Functions (GCC-O0)	ASM files
Binutils	2.37	16	5,465	107,098
Coreutils	9.0	106	2,321	47,406
Diffutils	3.8	4	592	12,008
Findutils	4.8.0	4	898	18,135
Tcpdump	4.9.3	1	1,448	32,243
Gmp	6.2.1	1	760	16,777
Curl	7.82.0	1	1,210	26,455
Total	-	133	12,694	260,122

**Compilation** We used two compilers (GCC-7.5 and Clang-10) with four optimization levels (O0/O1/O2/O3). In addition, the obfuscator Ollvm14 [64] was used to generate different obfuscated codes (sub/fla/bcf) with the four optimization levels, where “sub” denotes instruction substitution, “fla” denotes control flow flattening, “bcf” denotes bogus control flow. Thus, we got 11 different results for each of the input functions. It should be noted that all source codes were compiled with the option “*-fno-inline*” to avoid function inlining. The main reason is that the function inlining can interfere with similar function pairs, which is detrimental to the training of the model. After the compilation, we obtained 133 binaries for each compilation environment.

**Disassembly** UniASM is designed to generate embeddings for assembly codes. We disassembled the binaries with the help of Radare2 [65] and saved the functions in separate files. There is a slight difference in the number of functions obtained by disassembling the binary for different compilation options and code obfuscations. We got 12,694 unique functions (GCC-O0) and about 260K disassembly files.

**Similar function pairs** The training data for UniASM was constructed from similar function pairs. As shown in Table 2, we combined the disassembly results for each function to form 40 similar function pairs. The numbers in the table indicate the number of function pairs to be generated, “-” means no function pairs are generated. For the same compiler, only the optimization level needs to be considered, and there are six combinations (O0/O1, O0/O2, O0/O3, O1/O2, O1/O3, and O2/O3). For the different compilers, all 16 combinations were considered. For the code obfuscations, we only combined the obfuscated code with the normal code because we expected UniASM to learn the obfuscation features. We obtained about 500K similar function pairs in total.

**Table 2: Similar Function Pairs**

	GCC7.5	Clang10	Ollvm14-sub	Ollvm14-fla	Ollvm14-bcf
GCC7.5	6	16	-	-	-
Clang10	-	6	-	-	-
Ollvm14	-	-	4	4	4

**Dataset generation** We generated two sequences for each function pair according to the following steps:

1. Small functions with less than ten instructions were filtered to avoid semantically meaningless functions.
2. A new function pair was generated by swapping the two functions.
3. The tokenizer converted each function pair into a token sequence.
4. All the sequences were shuffled randomly and divided into two parts: 90% for training and 10% for validation.

The training dataset contains 428K sequences, and the validation dataset contains about 47K sequences.

#### 4.1.2 Evaluation Dataset

**Table 3: Projects Used for Evaluation (Dataset-1)**

Projects	Version	Binary	Functions (GCC-O0)	ASM files
libpcap	1.9.1	libpcap.so.1.9.1	532	5,105
libgd	2.1.1	libgd.so.3.0.0	445	4,403
libarchive	3.1.2	libarchive.so.14	1,656	15,461
openjpeg	2.1	libopenjp2.so.2.1.0	526	5,610
libav	12	libavformat.so.57.7.2	2,702	23,200
<b>Total</b>	-	-	<b>5,861</b>	<b>53,779</b>

This paper prepared three datasets to evaluate our model and the baselines:

**Dataset-1** is generated by five open-source projects, as shown in Table 3, and used for evaluating the performance of the models (Section 5.1). All these projects are not included in the training dataset and cover different application scenarios. The same software may have coding habits, functional characteristics, compilation environment, and other factors that may lead to information leakage in the test set, resulting in experimental result preference. Therefore, this paper uses binary programs that the training process has not seen as a test set to make the results more general. All projects were compiled by two compilers (GCC and Clang) with the four optimization levels (O0/O1/O2/O3) and by Ollvm14 with three obfuscations (sub/fla/bcf). We obtained 53,779 ASM files in total.

**Dataset-2** is a functions pool extracted randomly from Dataset-1 and used for ablation studies (Section 5.2). We randomly selected 200 functions from each project, resulting in 1000 functions. Since the projects were compiled in 11 different ways (as mentioned in Dataset-1), each function has 11 variants.

**Dataset-3** is a set of vulnerabilities and the affected projects, as shown in Table 5, and is used for evaluating performance on real-world vulnerability searching (Section 5.3). We selected eight vulnerabilities from a known vulnerabilities dataset [66] as the search targets. Then, we compiled the affected projects into 11 variants, like Dataset-1.

## 4.2 Baselines

We compared UniASM to the following six baselines:

**InnerEye [2]** uses LSTM in a Siamese architecture for binary code similarity detection. Specifically, it first leverages word2vec to generate instruction embedding and then feeds them to the Siamese architecture to learn basic block embedding. We obtained function embedding by taking the entire function as input. We used their official open-source code and pre-trained model [67] with its default parameters for evaluation.

**DeepBinDiff [55]** is a TADW-based model for basic block level diffing. It applies the CBOW model to generate the token embeddings and leverages the Text-associated DeepWalk (TADW) algorithm to learn basic block embedding from the inter-procedural control-flow graphs. Since DeepBinDiff is designed for basic block level comparison, we calculated the function embedding by averaging all basic block vectors of the function. The evaluation is based on the official implementation [68] and default parameters.

**Asm2vec [12]** is a PV-DM-based model for assembly language embedding. It uses random walks on the CFG to sample instruction sequences and then uses the PV-DM model to learn the embedding of the assembly language. The original paper of Asm2vec shows that their dataset contains function names of system libraries, but our validation dataset does not contain this kind of information. Asm2vec is not open source. We used an unofficial version [69] that is publicly available and configured the default parameters for evaluation.

**SAFE [14]** is an Attention-based model for assembly language embedding. It employs an RNN architecture with attention mechanisms to generate function embeddings. We used their official open-source code and pre-trained model [70] with its default parameters for evaluation.

**PalmTree [17]** is a BERT-based model for assembly instruction embedding. It uses three pre-training tasks to learn the characteristics of assembly instructions and generate the instruction embeddings. We used mean pooling to generate the function embeddings as the authors described in their paper. The evaluation is based on their official open-source code and pre-trained model [71] with its default parameters.

**jTrans [19]** is a jump-aware BERT-based model for assembly language embedding. It retains the jump relationships between instructions when generating input samples for BERT and allows BERT to learn the control flow information of the code. The official pre-trained model [72] was used with its default parameters for evaluation.

### 4.3 Evaluation Metrics

The task of function similarity search is often used to measure the performance of BCSD models. The function similarity search aims to find similar functions in a large pool of functions for the input function. The input function is selected from a source function pool, and the model searches the target function pool to find similar functions. The source and target function pools are defined as:

$$\mathcal{F}_{src} = \{f_1, f_2, \dots, f_i, \dots, f_n\}$$

$$\mathcal{G}_{dst} = \{g_{f_1}, g_{f_2}, \dots, g_{f_i}, \dots, g_{f_n}\}$$

The source function pool  $\mathcal{F}_{src}$  contains  $n$  functions, i.e., the pool size is  $n$ . Each input function  $f_i \in \mathcal{F}_{src}$  corresponds to a ground truth function  $g_{f_i} \in \mathcal{G}_{dst}$ .

The metric of Recall@k is used to evaluate the performance. We take the top- $k$  results for each query and sort them according to the similarity score. The Recall@ $k$  metric is the ratio of successful queries to the pool size (a successful query means the true ground function is in the top- $k$  results):

$$\text{Recall@}k(\mathcal{F}_{src}) = \frac{1}{|\mathcal{F}_{src}|} \sum_{f_i \in \mathcal{F}_{src}} \mathbb{I}[\text{Rank}(g_{f_i} | f_i) \leq k],$$

where  $\text{Rank}(g_{f_i} | f_i)$  refers to the ranking position of the first hit function for the  $i$ -th query.  $\mathbb{I}$  is an identity function that outputs 1 if the expression inside is evaluated to be true and 0 otherwise.

### 4.4 Hyperparameter Selection

We chose the following hyperparameters for UniASM: 4 transformer layers, 12 attention heads, max sequence length of 256, vocabulary size of 21000, and intermediate size of 3072. For training, we chose the batch size of 8, and the learning rate is set to 5e-5 with the warmup of 4 steps.

## 5 Evaluation

The evaluation aims to answer the following questions:

RQ1: How accurate is UniASM in BCSD tasks compared with other baselines? (Section 5.1)

RQ2: What impact do different backbone models, training tasks, serialization methods, tokenization algorithms, and sequence lengths have on the model’s accuracy in BCSD tasks? (Section 5.2)

RQ3: How effective is UniASM at searching known vulnerabilities? (Section 5.3)

All programs were compiled and pre-processed on an Ubuntu 20.04 server with 16GB RAM and Intel 8 core 3.0GHz CPU. In most cases, we used Radare2 for disassembling binary programs to generate assembly code. One of the baseline methods, jTrans, requires IDA pro [73] to disassemble the binary program. We trained UniASM on one TPU v3-8 chip, and all evaluation experiments were run on our laptop with Intel Core i7-9750H CPU, 32GB RAM, and NVIDIA GeForce GTX 1650 4GB GPU.

### 5.1 Performance

This paper evaluated UniASM and the baselines on three BCSD tasks: cross-compilers (X-COM, GCC-7.5/Clang-10), cross-optimization levels (X-OPT, O0/O1/O2/O3), and cross-obfuscations (X-OBF, sub/fla/bcf).

Table 4 shows the Recall@1 scores for UniASM and the baselines. The Recall@1 metric captures the ratio of functions correctly matched at the first position of the search results.

The evaluation dataset is Dataset-1, which is described in Section 4.1.2. There are five programs in Dataset-1, named libpcap, libgd, libarchive, openjpeg, and libav. We abbreviated them as P1, P2, P3, P4, and P5, as shown in the first column of Table 4.

**Table 4: BCSO Performance on Dataset-1**

Models	X-COM					X-OPT (GCC/Clang)							X-OBF				ALL	
	O0	O1	O2	O3	Avg.	O0&1	O0&2	O0&3	O1&2	O1&3	O2&3	Avg.	sub	fla	bef	Avg.		
P1	InnerEye	.06	.12	.13	.14	.11	.03/.04	.03/.03	.03/.03	.21/.34	.17/.33	.51/.62	.16/.23	.34	.18	.15	.22	.18
	DeepBinDiff	.13	.25	.18	.22	.20	.12/.07	.12/.06	.10/.07	.50/.47	.41/.49	.58/.68	.31/.31	.63	.33	.42	.46	.31
	Asm2Vec	.26	.33	.24	.29	.28	.11/.07	.11/.06	.10/.05	.49/.46	.41/.49	.61/.62	.31/.29	.59	.34	.22	.38	.31
	SAFE	.59	.56	.40	.45	.50	.36/.35	.31/.26	.28/.27	.64/.54	.50/.54	.68/.79	.46/.46	.76	.36	.33	.48	.47
	Palmtree	.21	.34	.36	.39	.33	.07/.03	.07/.04	.06/.04	.55/.52	.47/.53	.66/.73	.31/.32	.62	.27	.21	.37	.32
	jTrans	.43	.42	.41	.42	.42	.42/.34	.40/.28	.39/.30	.68/.63	.62/.62	.74/.77	.54/.49	.76	.54	.47	.59	.51
	<b>UniASM</b>	<b>.90</b>	<b>.78</b>	<b>.70</b>	<b>.69</b>	<b>.77</b>	<b>.76/.79</b>	<b>.74/.63</b>	<b>.64/.68</b>	<b>.83/.72</b>	<b>.72/.78</b>	<b>.77/.83</b>	<b>.74/.74</b>	<b>.91</b>	<b>.85</b>	<b>.74</b>	<b>.83</b>	<b>.76</b>
P2	InnerEye	.05	.15	.16	.16	.13	.05/.04	.04/.05	.03/.04	.19/.36	.18/.33	.56/.71	.18/.26	.31	.15	.14	.20	.19
	DeepBinDiff	.20	.27	.19	.21	.22	.14/.10	.11/.08	.12/.08	.49/.50	.43/.47	.66/.72	.33/.33	.65	.33	.44	.47	.33
	Asm2Vec	.33	.37	.39	.41	.38	.14/.10	.16/.11	.15/.13	.56/.59	.50/.57	.67/.76	.36/.38	.59	.32	.20	.37	.37
	SAFE	.56	.55	.45	.48	.51	.37/.35	.32/.28	.31/.28	.65/.66	.57/.65	.78/.90	.50/.52	.75	.29	.32	.45	.50
	Palmtree	.25	.43	.37	.38	.36	.08/.05	.08/.05	.07/.05	.65/.56	.55/.53	.74/.87	.36/.35	.58	.22	.20	.33	.35
	jTrans	.59	.52	.56	.56	.56	.53/.42	.51/.40	.50/.40	.77/.74	.74/.73	.81/.86	.64/.59	.84	.59	.52	.65	.61
	<b>UniASM</b>	<b>.82</b>	<b>.73</b>	<b>.67</b>	<b>.70</b>	<b>.73</b>	<b>.66/.67</b>	<b>.68/.60</b>	<b>.61/.61</b>	<b>.80/.71</b>	<b>.74/.71</b>	<b>.81/.91</b>	<b>.72/.70</b>	<b>.86</b>	<b>.72</b>	<b>.62</b>	<b>.73</b>	<b>.72</b>
P3	InnerEye	.02	.07	.10	.10	.07	.01/.01	.01/.01	.01/.02	.10/.30	.10/.29	.43/.63	.11/.21	.18	.08	.08	.11	.13
	DeepBinDiff	-	-	-	-	-	-	-	-	-	-	-	-	-	-	-	-	-
	Asm2Vec	.15	.25	.21	.23	.21	.06/.04	.05/.04	.04/.04	.42/.43	.35/.43	.55/.64	.25/.27	.42	.19	.13	.25	.25
	SAFE	.48	.47	.42	.40	.44	.25/.26	.21/.21	.17/.21	.55/.60	.46/.58	.68/.85	.39/.45	.65	.18	.20	.34	.41
	Palmtree	.15	.30	.29	.32	.27	.03/.02	.02/.02	.02/.02	.45/.48	.37/.47	.59/.75	.25/.29	.51	.15	.16	.27	.27
	jTrans	.37	.29	.28	.30	.31	.25/.20	.23/.17	.23/.17	.60/.57	.53/.56	.65/.74	.42/.40	.72	.43	.36	.50	.40
	<b>UniASM</b>	<b>.82</b>	<b>.73</b>	<b>.72</b>	<b>.72</b>	<b>.75</b>	<b>.67/.73</b>	<b>.64/.60</b>	<b>.56/.58</b>	<b>.76/.72</b>	<b>.67/.70</b>	<b>.73/.89</b>	<b>.67/.70</b>	<b>.84</b>	<b>.71</b>	<b>.60</b>	<b>.72</b>	<b>.72</b>
P4	InnerEye	.05	.13	.15	.15	.12	.03/.02	.03/.02	.03/.02	.21/.42	.18/.40	.59/.77	.18/.28	.23	.20	.11	.18	.20
	DeepBinDiff	.15	.18	.09	.12	.14	.12/.10	.09/.07	.11/.08	.42/.43	.40/.42	.56/.65	.28/.29	.51	.37	.31	.40	.27
	Asm2Vec	.29	.31	.28	.30	.30	.11/.07	.10/.06	.09/.06	.46/.47	.39/.46	.60/.60	.29/.29	.50	.38	.17	.35	.30
	SAFE	.59	.55	.49	.50	.53	.39/.31	.34/.29	.32/.29	.69/.69	.63/.68	.83/.94	.53/.53	.77	.46	.28	.50	.53
	Palmtree	.26	.46	.50	.52	.44	.07/.03	.06/.04	.04/.05	.65/.62	.56/.61	.75/.89	.36/.37	.59	.38	.16	.38	.38
	jTrans	.50	.40	.45	.44	.45	.42/.37	.40/.33	.42/.33	.78/.69	.74/.69	.83/.89	.60/.55	.80	.67	.42	.63	.56
	<b>UniASM</b>	<b>.85</b>	<b>.77</b>	<b>.80</b>	<b>.81</b>	<b>.81</b>	<b>.71/.68</b>	<b>.69/.62</b>	<b>.65/.62</b>	<b>.89/.78</b>	<b>.84/.77</b>	<b>.85/.95</b>	<b>.77/.74</b>	<b>.87</b>	<b>.81</b>	<b>.61</b>	<b>.76</b>	<b>.77</b>
P5	InnerEye	.02	.05	.07	.06	.05	.01/.01	.01/.01	.01/.01	.12/.38	.11/.34	.65/.78	.15/.26	.01	.07	.07	.05	.15
	DeepBinDiff	-	-	-	-	-	-	-	-	-	-	-	-	-	-	-	-	-
	Asm2Vec	.11	.26	.25	.27	.22	.05/.03	.05/.03	.04/.03	.53/.60	.47/.58	.73/.84	.31/.35	.03	.19	.10	.11	.27
	SAFE	.27	.43	.39	.40	.37	.15/.12	.13/.10	.13/.10	.57/.68	.52/.66	.79/.94	.38/.43	.11	.15	.17	.14	.36
	Palmtree	.10	.31	.41	.42	.31	.03/.02	.02/.02	.03/.02	.61/.65	.54/.63	.78/.91	.34/.38	.02	.12	.12	.09	.30
	jTrans	.45	.32	.35	.33	.36	.31/.24	.31/.25	.32/.24	.79/.79	.75/.77	.83/.93	.55/.54	.34	.60	.41	.45	.49
	<b>UniASM</b>	<b>.82</b>	<b>.76</b>	<b>.77</b>	<b>.77</b>	<b>.78</b>	<b>.63/.58</b>	<b>.57/.49</b>	<b>.52/.48</b>	<b>.86/.80</b>	<b>.80/.78</b>	<b>.83/.95</b>	<b>.70/.68</b>	<b>.49</b>	<b>.68</b>	<b>.52</b>	<b>.56</b>	<b>.69</b>

### 5.1.1 Empirical Results for Cross Compilers (X-COM)

In this evaluation, we generated function pools for each optimization level. The function pools of GCC were used as the source pools of searching, while the pools of Clang were used as the target pools. As shown in the column “X-COM” of Table 3, there are four searching tasks: “O0” is short for “GCC-O0 vs. Clang-O0,” “O1” is short for “GCC-O1 vs. Clang-O1,” etc. UniASM achieved average Recall@1 scores of 0.77, while the closest baseline competitor (SAFE) achieved 0.47. UniASM outperforms it by 64%.

### 5.1.2 Empirical Results for Cross Optimization Levels (X-OPT)

In this evaluation, we compared the four optimization levels in pairs, resulting in six searching tasks, as shown in column “X-OPT” of Table 3. We did this evaluation for GCC and Clang, respectively. “O0&1” is short for “GCC-O0 vs. GCC-O1/Clang-O0 vs. Clang-O1,” “O0&2” is short for “GCC-O0 vs. GCC-O2/Clang-O0 vs. Clang-O2,” etc. The left of the two scores in the cell is for GCC, and the right is for Clang. UniASM outperforms the baseline models in most of the tasks. Our model seems more efficient in solving more challenging BCSO tasks, such as O0&O3. In the most challenging task, “Clang-O0 vs. Clang-O3,” UniASM still achieved an average Recall@1 score of 0.59, while the closest baseline (jTrans) achieved 0.29.

### 5.1.3 Empirical Results for Cross Obfuscations (X-OBF)

In this evaluation, the source pool is the non-obfuscated functions, and the pools of the three obfuscation types were used as the target pools. As shown in the column “X-OBF” of Table 3, there are three searching tasks: “sub,” “fla,” and “bcf,” which stand for “Ollvm-none vs. Ollvm-sub,” “Ollvm-none vs. Ollvm-fla,” and “Ollvm-none vs. Ollvm-bcf.” UniASM achieved an average Recall@1 score of 0.72, outperforming its closest baseline competitor (jTrans) by 29%.

## 5.2 Ablation Studies

In the ablation studies, we try to find the factors that affect the model’s performance on BCSD. We evaluated the performance of different backbone models (Section 5.2.1), training tasks (Section 5.2.2), function serialization methods (Section 5.2.3), tokenization algorithms (Section 5.2.4), and max sequence lengths (Section 5.2.5) on three typical BCSD tasks: X-OPT (GCC-O0 vs. GCC-O3), X-COM (GCC-O3 vs. Clang-O3), and X-OBF (Ollvm-none vs. Ollvm-bcf). In addition, we compared the embedding space layout of different models to demonstrate their differences visually (Section 5.2.6).

We used the Recall@k metric to evaluate the performance of the models. To ensure the fairness of the experiments, we configured all the models with the same hyperparameters (Section 4.4) and used the same training and evaluation datasets (Section 4.1). The evaluation dataset is Dataset-2, which is a collection of 1,000 functions from different programs.

### 5.2.1 Backbone Models

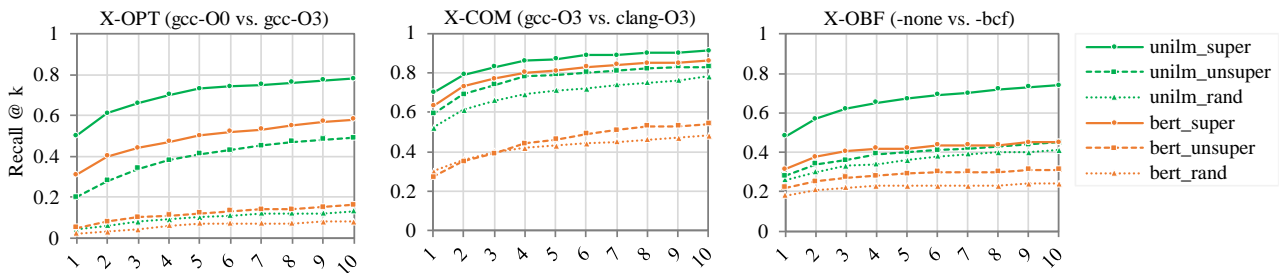


Figure 5: Performance of different models

UniASM is based on the UniLM model, and the BERT model is used as a competitor, which is used in PalmTree and jTrans. Since BCSD take the embeddings of binary code for searching task, in this study, we evaluated the performance of embeddings generated by the two models in three BCSD tasks. To more comprehensively demonstrate the differences between the two models, we designed three different training scenarios:

- 1) **Random parameters:** We evaluated BERT and UniLM with the initial random parameters (“bert\_rand” and “unilm\_rand” in Figure 5) to figure out the baseline performance of the models.
- 2) **Unsupervised learning:** We applied only MLM to implement unsupervised training of the two models (“bert\_unsuper” and “unilm\_unsuper” in Figure 5). MLM is BERT’s default training task, which randomly masks 15% of the tokens in each sequence and trains the model to predict the missing words based on the context.
- 3) **Supervised learning:** SFP was applied to implement supervised training of the two models (“bert\_super” and “unilm\_super” in Figure 5). SFP is designed to train the model to determine whether two functions are similar.

The results show that UniLM performs much better than BERT in all the tasks. Both supervised and unsupervised training can improve the performance of the models in the BCSO tasks. We are surprised that UniLM, even with randomly initialized parameters, outperforms the unsupervised trained BERT model in both X-COM and X-OBF tasks.

### 5.2.2 Training Tasks

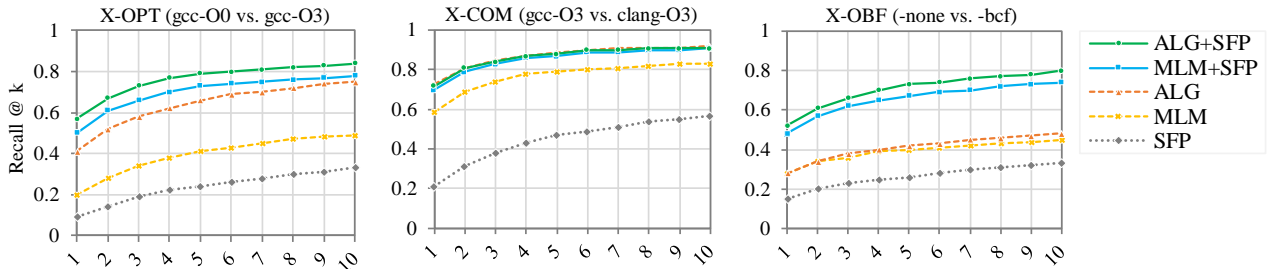


**Figure 6:** Performance of different training tasks

In this study, we first trained UniASM with one training task at a time, resulting in three pre-trained models: MLM, ALG, and SFP. In addition, we evaluated the combinations of the training tasks, resulting in another two pre-trained models: MLM+SFP and ALG+SFP. We have not tested the combination of MLM and ALG due to the fact that both of them are masking methods with different strategies: MLM implements random position masking, while ALG implements masking of the second half of the sentence.

As shown in Figure 6, the model with ALG+SFP tasks outperforms all other competitors. When observing the resulting data closely, we find some interesting details:

- ALG shows high performance in both X-OPT and X-COM. However, the performance in X-OBF is relatively poor. As shown in Figure 6, ALG improves performance over MLM by an average of 66% in X-OPT and 14% in X-COM, but only 5% in X-OBF.
- SFP task performs poorly in all BCSO tasks. However, it can significantly improve the model’s performance when combined with MLM or ALG. For the X-OBF task, SFP improves the average Recall@k of MLM from 0.39 to 0.66 and the average Recall@k of ALG from 0.41 to 0.71.

The experimental results indicate that ALG is more suitable for BCSO than MLM. One possible reason is that ALG makes the model more focused on the overall semantics of the whole function, while MLM aims to find the missing instructions.

### 5.2.3 Function Serialization Methods

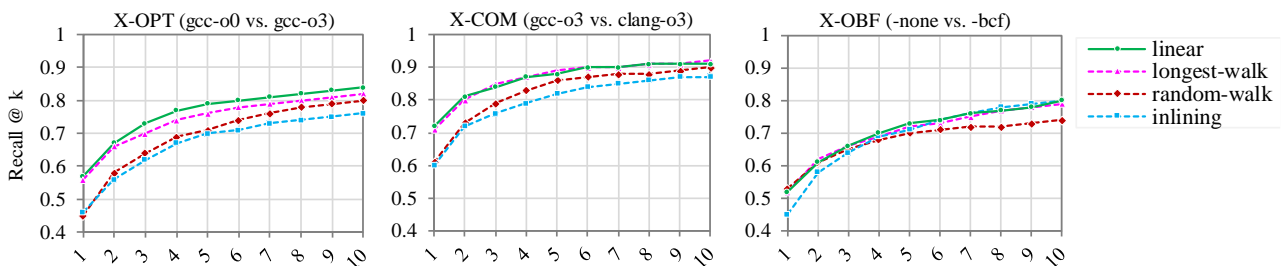


**Figure 7:** Performance of different serialization methods

Function serialization aims to serialize a function to a sequence, which can then be tokenized and fed to the NLP model. In this study, we prepared three different serialization methods and also tested the inlining compilation:

- 1) **Linear (Our approach):** The assembly function in the training dataset was compiled with the no-inlining option “*-fno-inline,*” and the function was serialized in linear order (the address order). The linear approach can make the generated sequence contain as many instructions as possible.
- 2) **Random-walk:** Random-walk, as used in Asm2Vec, chooses a random path on the CFG of a function, which can extract structure information of the function. The disadvantages are that the randomness leads to the instability of the sequence content, and extracting one execution path of the function shortens the generated sequence’s length.
- 3) **Longest-walk:** Longest-walk is an optimized version of random-walk, which chooses the longest path on the CFG of a function. A longer path contains more semantic information about a function. However, it still faces the same problem as random-walk: it can only extract one execution path of the function, which loses some semantics of the function.
- 4) **Inlining compilation:** Inlining is the default feature of the compiler, which eliminates call-linkage overhead and can expose other optimization opportunities. Since the evaluation dataset was compiled with default options (inlining turn-on), we designed this experiment to find out whether training with the inlining functions will lead to better performance. However, the new training dataset has 32% fewer functions than before because some functions are inlined into another function.

Surprisingly, the path-based methods (random-walk and longest-walk) did not outperform the default linear method, as shown in Figure 7. Regarding this phenomenon, we believe that there are some possible explanations:

- First, the sequence generated by the linear order can contain more instructions. According to our statistics, the average instruction count of the linear method is 148, while it is 39 and 62 for random-walk and longest-walk.
- Second, the linear order already largely implies the execution order of the function because the instructions in the same basic block are in the right position.
- Third, the deep learning model can somewhat adapt to the different order of basic blocks. The control flow instructions, such as *jmp*, can give a hint to the model.

We also find that the inlining dataset is worse than the default dataset. The possible reason is that function inlining reduces the similarity of the function pairs, which makes the training more difficult.

#### 5.2.4 Tokenization Algorithms

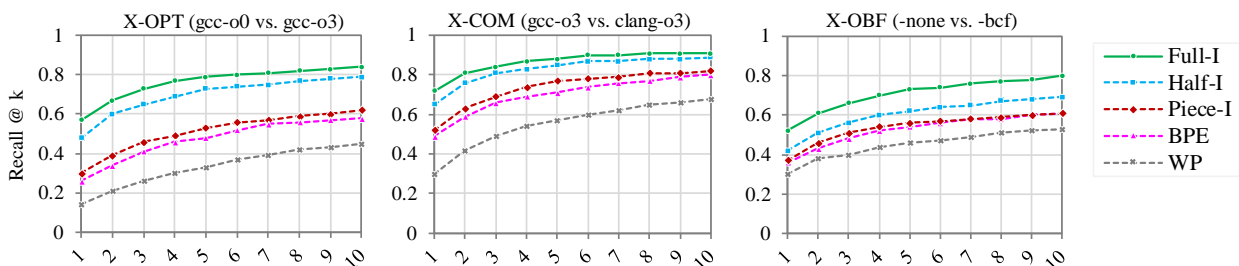


**Figure 8:** Performance of different tokenization algorithms

Tokenization is an important step in data preprocessing, which convert the raw instructions to tokens. In this study, we evaluated three tokenization methods (Full-Instruction, Half-Instruction, and Piece-Instruction)



designed for assembly code and two tokenization methods (Byte-Pair Encoding [74] and Word-Piece [75]) designed for natural language.

- 5) **Full-Instruction (Full-I, our approach):** Full-I takes a single instruction as a token, as detailed in Section 3.2.2. Due to the limitation of input size by the backbone model, coarse-grained tokenization means that more instructions can be used to represent learning. The disadvantage is that it leads to a larger vocabulary and is more prone to the OOV problem.
- 6) **Half-Instruction (Half-I):** Half-I splits each instruction into two parts: the opcode and the operands. For example, the instruction “*mov rax, [rbx+NUM]*” can be tokenized into two tokens: “*mov*” and “*rax\_[rbx+NUM]*.” This approach can reduce the vocabulary while preserving the semantic information of the operands. However, the sequence size of a function may be twice of Full-I, which may cause the input length to exceed the limit of the model.
- 7) **Piece-Instruction (Piece-I):** Piece-I is used by jTrans, DeepBinDiff, and PalmTree. It is more fine-grained than Full-I and Half-I. Each word in the instruction was treated as a token instead of the whole instruction. For example, the instruction “*mov rax, [rbx+NUM]*” can be tokenized into four tokens: “*mov,*” “*rax,*” “*rbx,*” and “*NUM.*” Piece-I is easy to implement and can effectively alleviate OOV problem. However, it destroys the integrity of instructions and increases the difficulty of representation learning. What’s worse, it increases the serialization length of the functions, leading to a higher truncation rate.
- 8) **Byte-Pair Encoding (BPE):** BPE relies on a pre-tokenizer that splits the sentence into words. Since BPE is designed for natural language, we concatenate all the instructions of a function into a sentence, separated by spaces. According to this, BPE can easily encode a function into a token sequence.
- 9) **Word-Piece (WP):** WP is the sub-word tokenization algorithm used for BERT, similar to BPE. WP only differs slightly in its symbol pair selection strategy compared to BPE. We prepare the sentences in the same way as for BPE and train WP based on them.

The evaluation results show that Full-I outperforms all other methods. According to the results, we find that coarse-grained tokenization can achieve better performance. Since BPE and WP are all fine-grained tokenization methods, they perform poorly, as expected. The experimental results also indicate that the OOV problem may not be the main factor affecting the embedding performance, and the semantics in the sequence plays a more critical role. However, Full-I requires a vocabulary of over 20,000, while Half-I and Piece-I only need about 7,000 and 4,000, respectively.

### 5.2.5 Max Sequence Lengths

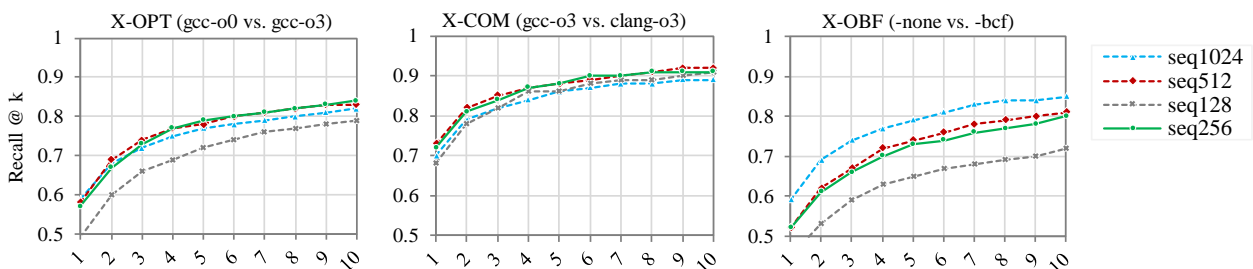


**Figure 9:** Performance of different max sequence lengths

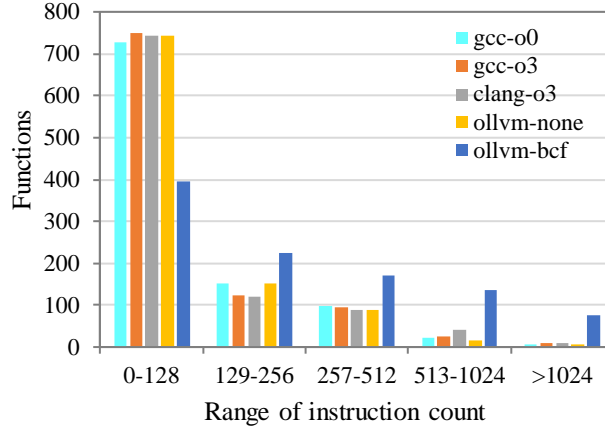


**Figure 10:** Functions with different instruction count

The max sequence length (MaxSL) is a hyperparameter of the model that limits the maximum length of a single input. According to our experience, if the MaxSL is too short, the input will be truncated, which can negatively impact the performance of representation learning. Conversely, if the MaxSL is too long, it will increase the cost of both model training and usage. In this study, we evaluated four different MaxSLs: Seq128, Seq256, Seq512, and Seq1024.

The results show that Seq128 performs worse than the others in all tasks, and Seq1024 performs significantly better than the others only in the X-OBF task. The possible reason for this phenomenon is that the input length did not exceed the MaxSL. To verify it, we counted the number of instructions in the functions in Dataset-2 used in this study. As shown in Figure 10, all functions were placed into five buckets based on their instruction counts: [0-128], [129-256], [257-512], [513-1024], and [>1024]. We find that about 35% of the functions contain more than 128 instructions, which makes Seq-128 suffer a serious truncation problem, resulting in decreased performance. However, only about 12% of the functions contain more than 256 instructions, making Seq256, Seq512, and Seq1024 perform similarly in X-OPT and X-COM tasks. For the X-OBF task, the BCF obfuscation algorithm inserts bogus control flow into the functions. The increased number of instructions enables Seq1024 to leverage its advantages better.

In summary, longer MaxSL has an advantage in handling larger functions. According to the statistics, most functions contain fewer than 256 instructions. Therefore, this paper uses Seq256 as the default MaxSL, which can achieve acceptable performance at a lower cost.

### 5.2.6 Embedding Space Analysis

The function embeddings were all generated from Dataset-1. We compared BERT and UniASM with different training tasks to show the impact of the tasks. “-random” means that the model uses the initial random parameters. In addition, four best-performing baseline models (Asm2Vec, SAFE, Palmtree, and jTrans) were selected for comparison. We leveraged t-SNE [76] to visualize the high-dimensional vectors. Each color indicates one compilation environment.

When calculating similarity, we want similar embeddings to be as close as possible and different embeddings as far as possible. As all functions of a compilation environment (the points in the same color) are considered different, a good embedding space should make the points uniformly distributed.

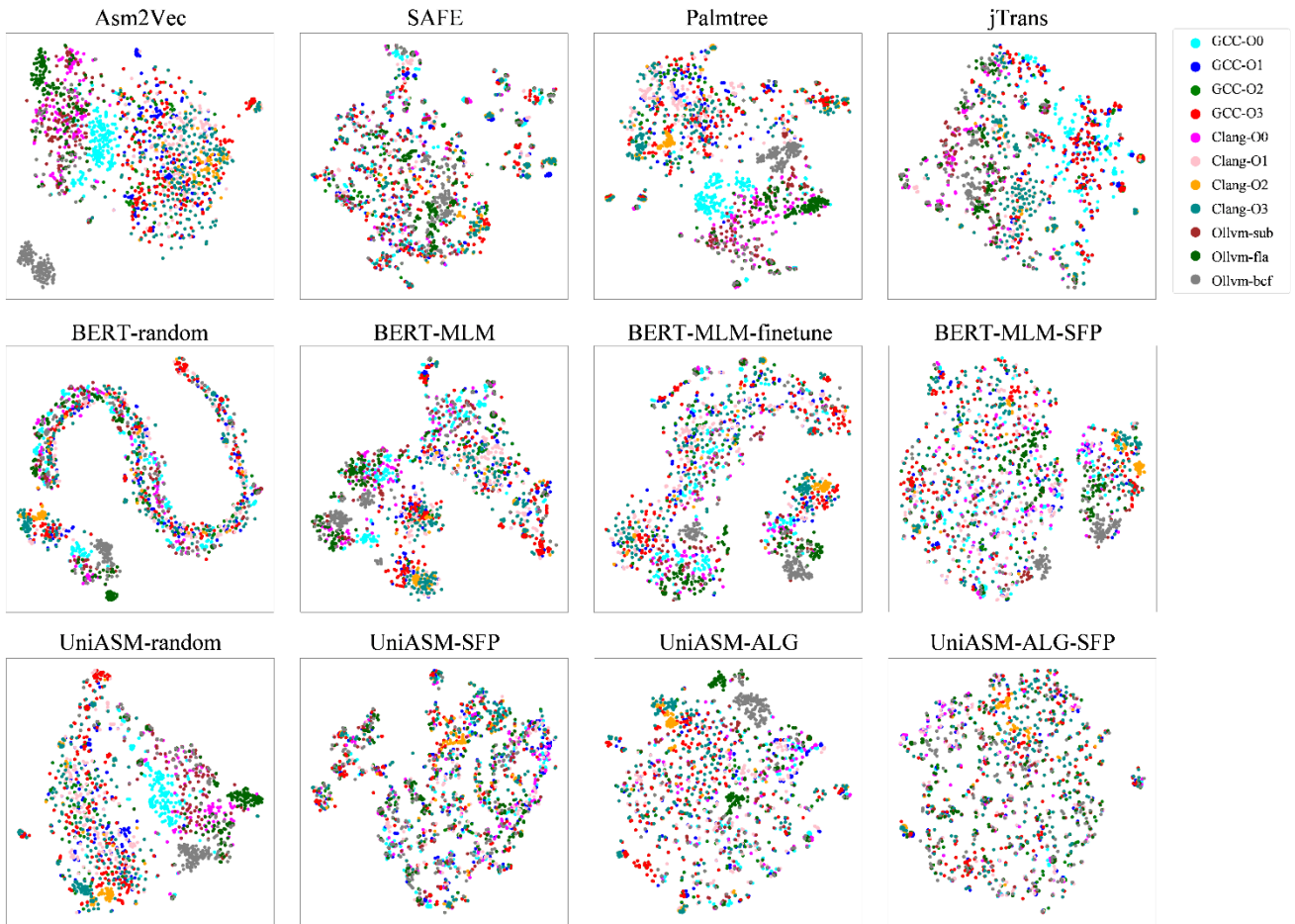


**Figure 11:** Embedding space of different models

As shown in Figure 11, the embeddings of UniASM are more uniformly distributed than BERT, which explains why UniASM performs better than BERT. The embedding spaces have significant differences when UniASM is trained with different tasks. Applying SFP alone does not distinguish the embeddings very well. ALG does better, but there are still some local clusters. The joint task ALG+SFP makes most of the embeddings uniformly distributed. It is worth mentioning that BERT-MLM-finetune is the BERT model fine-tuned by a similarity classification task. According to our testing, although it can handle classification tasks well, the generated function embeddings perform poorly in BCSD tasks. Overall, the results of this study are very consistent with the previous evaluation results.

### 5.3 Vulnerability Searching

Vulnerability searching is one of the main applications in computer security. This evaluation compared UniASM’s performance with four best-performing baseline models (Asm2Vec, SAFE, Palmtree, and jTrans). The evaluation dataset is dataset-3, detailed in Section 4.1.2. For each vulnerability query, the source function pool is the 11 vulnerable function variants, and the target function pool is all functions in all variants. The size of the target function pool for each project varies from 4,296 to 96,836. For example, the target function pool of CVE-2013-1944 from the curl-7.29.0 project contains 8334 functions.

As the source pool contains 11 vulnerable functions, we query each function in the target function pool and collect the top-11 results. Recall@11 was used as the evaluation metric, meaning the model retrieves how many

vulnerable functions in the top-11 results. We calculated the mean Recall@11 for all 11 queries. As shown in Table 5, UniASM outperforms all baseline models, and its score is 29% to 207% higher than the leading baseline.

**Table 5:** Performance on Vulnerability Searching

Vulnerability	Software	Pool	Models (Mean Recall@11)				
			Asm2vec	SAFE	PalmTree	jTrans	UniASM
CVE-2013-1944	curl-7.29.0	8334	.16	.27	.14	.27	<b>.77</b>
CVE-2015-8877	libgd-2.1.1	4296	.33	.36	.22	.36	<b>.69</b>
CVE-2016-1541	libarchive-3.1	15125	.25	.22	.22	.28	<b>.86</b>
CVE-2016-7163	openjpeg-2.1	4804	.17	.38	.26	.24	<b>.45</b>
CVE-2016-8858	openssh-7.3	53454	.12	.21	.16	.23	<b>.42</b>
CVE-2017-9051	libav-12	23048	.21	.21	.20	.38	<b>.54</b>
CVE-2017-7866	ffmpeg-2.8.6	96836	.21	.36	.36	.28	<b>.52</b>
CVE-2018-8970	libressl-2.7.0	50762	.21	.27	.21	.18	<b>.35</b>

## 6 Limitations

In this section, we discuss some limitations of our model:

**Cross-Architecture** As the training dataset of UniASM consists of x86\_64 code. Our pre-trained model can only be used for x86\_64 binaries. However, UniASM is not limited to this and can be re-trained with the dataset of other architectures (e.g., ARM, MIPS, etc.).

**Control flow semantics** UniASM performs linear serialization of functions, so the current model cannot learn the control flow semantics. Although our ablation studies show that the linear one is similar to the random-walk or the longest-walk. Existing work, such as jTrans, shows that control flow information is an important semantic component of functions. A reasonable representation of the control flow should be helpful and deserves further study.

**Out-of-vocabulary** Our tokenizer treats the whole instruction as a token, which makes the token contain more semantics information. However, a more complex token means a larger dictionary, leading to the OOV problem. In this paper, UniASM tries to mitigate the OOV problem by normalizing the instructions.

## 7 Conclusion and Future Work

In this paper, we propose UniASM, the first attempt to apply an UniLM-based model to BCSD with two fine-designed training tasks. UniASM learns the semantics of assembly code and generates the function embeddings. The generated vectors can be used directly for similarity comparisons without fine-tuning. Experimental results show that UniASM has better performance than the top-performing baselines. In addition, we conduct ablation studies to explore the factors that affect the model’s accuracy in BCSD tasks.

ALG gives the model the ability to generate assembly code. In the future, we plan to apply this ability to more valuable downstream tasks, such as code transformation, automatic coding, etc.

## References

- [1] B. Liu, W. Huo, C. Zhang, W. Li, F. Li, A. Piao, and W. Zou, “ $\alpha$ diff: Cross-version binary code similarity detection with dnn,” in Proceedings of the 33rd ACM/IEEE International Conference on Automated Software Engineering, ASE 2018, Montpellier, France, September 3-7, 2018. ACM, 2018, pp. 667–678.
- [2] F. Zuo, X. Li, Z. Zhang, P. Young, L. Luo, and Q. Zeng, “Neural machine translation inspired binary code similarity comparison beyond function pairs,” in 26th Annual Network and Distributed System Security Symposium, NDSS 2019, San Diego, California, USA, February 24-27, 2019. The Internet Society, 2019.
- [3] S. Cesare and Y. Xiang, “Malware variant detection using similarity search over sets of control flow graphs,” in IEEE 10th International Conference on Trust, Security and Privacy in Computing and Communications, TrustCom 2011, Changsha, China, 16-18 November, 2011. IEEE Computer Society, 2011, pp. 181–189.
- [4] S. Cesare, Y. Xiang, and W. Zhou, “Control flow-based malware variant detection,” IEEE Transactions on Dependable and Secure Computing, vol. 11, pp. 307–317, 2014.
- [5] C. Tamas, D. Papp, and L. Buttyan, “Simbiota: Similarity-based malware detection on iot devices,” in Proceedings of the 6th International Conference on Internet of Things, Big Data and Security, IoTBDS 2021, Online Streaming, April 23-25, 2021. SCITEPRESS, 2021, pp. 58–69.
- [6] Y. Hu, Y. Zhang, J. Li, and D. Gu, “Binary code clone detection across architectures and compiling configurations,” in Proceedings of the 25th International Conference on Program Comprehension, ICPC 2017, Buenos Aires, Argentina, May 22-23, 2017. IEEE Computer Society, 2017, pp. 88–98.
- [7] S. H. H. Ding, B. C. M. Fung, and P. Charland, “Kam1n0: Map reduce-based assembly clone search for reverse engineering,” in Proceedings of the 22nd ACM SIGKDD International Conference on Knowledge Discovery and Data Mining, San Francisco, CA, USA, August 13-17, 2016. ACM, 2016, pp. 461–470.
- [8] Z. Xu, B. Chen, M. Chandramohan, Y. Liu, and F. Song, “Spain: Security patch analysis for binaries towards understanding the pain and pills,” in Proceedings of the 39th International Conference on Software Engineering, ICSE 2017, Buenos Aires, Argentina, May 20-28, 2017. IEEE / ACM, 2017, pp. 462–472.
- [9] A. Sæbjørnsen, J. Willcock, T. Panas, D. J. Quinlan, and Z. Su, “Detecting code clones in binary executables,” in Proceedings of the Eighteenth International Symposium on Software Testing and Analysis, ISSTA 2009, Chicago, IL, USA, July 19-23, 2009. ACM, 2009, pp. 117–128.
- [10] Y. Ji, L. Cui, and H. H. Huang, “Buggraph: Differentiating source binary code similarity with graph triplet-loss network,” in ASIA CCS ’21: ACM Asia Conference on Computer and Communications Security, Virtual Event, Hong Kong, June 7-11, 2021. ACM, 2021, pp. 702–715.
- [11] X. Xu, C. Liu, Q. Feng, H. Yin, L. Song, and D. X. Song, “Neural network-based graph embedding for cross-platform binary code similarity detection,” in Proceedings of the 2017 ACM SIGSAC Conference on Computer and Communications Security, CCS 2017, Dallas, TX, USA, October 30 - November 03, 2017. ACM, 2017, pp. 363–376.
- [12] S. H. H. Ding, B. C. M. Fung, and P. Charland, “Asm2vec: Boosting static representation robustness for binary clone search against code obfuscation and compiler optimization,” in 2019 IEEE Symposium on Security and Privacy, SP 2019, San Francisco, CA, USA, May 19-23, 2019. IEEE, 2019, pp. 472–489.
- [13] Q. V. Le and T. Mikolov, “Distributed representations of sentences and documents,” in Proceedings of the 31th International Conference on Machine Learning, ICML 2014, Beijing, China, 21-26 June 2014, ser. JMLR Workshop and Conference Proceedings, vol. 32. JMLR.org, 2014, pp. 1188–1196.
- [14] L. Massarelli, G. A. D. Luna, F. Petroni, L. Querzoni, and R. Baldoni, “Safe: Self-attentive function embeddings for binary similarity,” in Detection of Intrusions and Malware, and Vulnerability Assessment - 16th International

Conference, DIMVA 2019, Gothenburg, Sweden, June 19-20, 2019, Proceedings, ser. Lecture Notes in Computer Science, vol. 11543. Springer, 2019, pp. 309–329.

- [15] TensorFlow, “Word2vec skip-gram implementation in tensorflow,” <https://tensorflow.google.cn/tutorials/text/word2vec>, 2022.
- [16] Z. Lin, M. Feng, C. N. dos Santos, M. Yu, B. Xiang, B. Zhou, and Y. Bengio, “A structured self-attentive sentence embedding,” in 5th International Conference on Learning Representations, ICLR 2017, Toulon, France, April 24-26, 2017, Conference Track Proceedings. OpenReview.net, 2017.
- [17] X. Li, Q. Yu, and H. Yin, “Palmtree: Learning an assembly language model for instruction embedding,” in CCS ’21: 2021 ACM SIGSAC Conference on Computer and Communications Security, Virtual Event, Republic of Korea, November 15 - 19, 2021. ACM, 2021, pp. 3236–3251.
- [18] J. Devlin, M.-W. Chang, K. Lee, and K. Toutanova, “Bert: Pretraining of deep bidirectional transformers for language understanding,” in proceedings of the 2019 Conference of the North American Chapter of the Association for Computational Linguistics: Human Language Technologies, NAACL-HLT 2019, Minneapolis, MN, USA, June 2-7, 2019, Volume 1. Association for Computational Linguistics, 2019, pp. 4171–4186.
- [19] H. Wang, W. Qu, G. Katz, W. Zhu, Z. Gao, H. Qiu, J. Zhuge, and C. Zhang, “jTrans: jump-aware transformer for binary code similarity detection,” in ISSTA ’22: 31st ACM SIGSOFT International Symposium on Software Testing and Analysis, Virtual Event, South Korea, July 18 - 22, 2022. ACM, 2022, pp. 1–13.
- [20] D. Gao, M. K. Reiter, and D. X. Song, “Binhunt: Automatically finding semantic differences in binary programs,” in Information and Communications Security, 10th International Conference, ICICS 2008, Birmingham, UK, October 20-22, 2008, Proceedings, ser. Lecture Notes in Computer Science, vol. 5308. Springer, 2008, pp. 238–255.
- [21] J. Ming, M. Pan, and D. Gao, “iBinhunt: Binary hunting with inter-procedural control flow,” in Information Security and Cryptology - ICISC 2012 - 15th International Conference, Seoul, Korea, November 28-30, 2012, Revised Selected Papers, ser. Lecture Notes in Computer Science, vol. 7839. Springer, 2012, pp. 92–109.
- [22] M. Egele, M. Woo, P. Chapman, and D. Brumley, “Blanket execution: Dynamic similarity testing for program binaries and components,” in Proceedings of the 23rd USENIX Security Symposium, San Diego, CA, USA, August 20-22, 2014. USENIX Association, 2014, pp. 303–317.
- [23] M. Chandramohan, Y. Xue, Z. Xu, Y. Liu, C. Y. Cho, and H. B. K. Tan, “Bingo: cross-architecture cross-os binary search,” in Proceedings of the 24th ACM SIGSOFT International Symposium on Foundations of Software Engineering, FSE 2016, Seattle, WA, USA, November 13-18, 2016. ACM, 2016, pp. 678–689.
- [24] Y. Xue, Z. Xu, M. Chandramohan, and Y. Liu, “Accurate and scalable cross-architecture cross-os binary code search with emulation,” *IEEE Trans. Software Eng.*, vol. 45, no. 11, pp. 1125–1149, 2019.
- [25] J. Pewny, B. Garmany, R. Gawlik, C. Rossow, and T. Holz, “Cross-architecture bug search in binary executables,” *Information Technology*, vol. 59, pp. 83–91, 2015.
- [26] Y. Hu, H. Wang, Y. Zhang, B. Li, and D. Gu, “A semantics-based hybrid approach on binary code similarity comparison,” *IEEE Trans. Software Eng.*, vol. 47, no. 6, pp. 1241–1258, 2021.
- [27] S. Wang and D. Wu, “In-memory fuzzing for binary code similarity analysis,” in Proceedings of the 32nd IEEE/ACM International Conference on Automated Software Engineering, ASE 2017, Urbana, IL, USA, October 30 - November 03, 2017. IEEE Computer Society, 2017, pp. 319–330.
- [28] J. Ming, D. Xu, Y. Jiang, and D. Wu, “Binsim: Trace-based semantic binary diffing via system call sliced segment equivalence checking,” in 26th USENIX Security Symposium, USENIX Security 2017, Vancouver, BC, Canada, August 16-18, 2017. USENIX Association, 2017, pp. 253–270.

- [29] Hex-rays, “Flirt,” <https://hex-rays.com/products/ida/tech/flirt/>, 2022.
- [30] E. R. Jacobson, N. E. Rosenblum, and B. P. Miller, “Labeling library functions in stripped binaries,” in Proceedings of the 10th ACM SIGPLAN-SIGSOFT workshop on Program analysis for software tools, PASTE’11, Szeged, Hungary, September 5-9, 2011. ACM, 2011, pp. 1–8.
- [31] M. R. Farhadi, B. C. M. Fung, P. Charland, and M. Debbabi, “Binclone: Detecting code clones in malware,” in Eighth International Conference on Software Security and Reliability, SERE 2014, San Francisco, California, USA, June 30 - July 2, 2014. IEEE, 2014, pp. 78–87.
- [32] J. Jang, M. Woo, and D. Brumley, “Towards automatic software lineage inference,” in Proceedings of the 22th USENIX Security Symposium, Washington, DC, USA, August 14-16, 2013. USENIX Association, 2013, pp. 81–96.
- [33] X. Hu, K. G. Shin, S. Bhatkar, and K. Griffin, “Mutantx-s: Scalable malware clustering based on static features,” in 2013 USENIX Annual Technical Conference, San Jose, CA, USA, June 26-28, 2013. USENIX Association, 2013, pp. 187–198.
- [34] L. Nouh, A. Rahimian, D. Mouheb, M. Debbabi, and A. Hanna, “Binsign: Fingerprinting binary functions to support automated analysis of code executables,” in ICT Systems Security and Privacy Protection - 32nd IFIP TC 11 International Conference, SEC 2017, Rome, Italy, May 29-31, 2017, Proceedings, ser. IFIP Advances in Information and Communication Technology, vol. 502. Springer, 2017, pp. 341–355.
- [35] P. Shirani, L. Wang, and M. Debbabi, “Binshape: Scalable and robust binary library function identification using function shape,” in Detection of Intrusions and Malware, and Vulnerability Assessment- 14th International Conference, DIMVA 2017, Bonn, Germany, July 6-7, 2017, Proceedings, ser. Lecture Notes in Computer Science, vol. 10327. Springer, 2017, pp. 301–324.
- [36] Y. David and E. Yahav, “Tracelet-based code search in executables,” in ACM SIGPLAN Conference on Programming Language Design and Implementation, PLDI ’14, Edinburgh, United Kingdom -June 09 - 11, 2014. ACM, 2014, pp. 349–360.
- [37] H. Huang, A. M. Youssef, and M. Debbabi, “Binsequence: Fast, accurate and scalable binary code reuse detection,” in Proceedings of the 2017 ACM on Asia Conference on Computer and Communications Security, AsiaCCS 2017, Abu Dhabi, United Arab Emirates, April 2-6, 2017. ACM, 2017, pp. 155–166.
- [38] J. Powny, F. Schuster, L. Bernhard, T. Holz, and C. Rossow, “Leveraging semantic signatures for bug search in binary programs,” in Proceedings of the 30th Annual Computer Security Applications Conference, ACSAC 2014, New Orleans, LA, USA, December 8-12, 2014. ACM, 2014, pp. 406–415.
- [39] Q. Feng, M. Wang, M. Zhang, R. Zhou, A. Henderson, and H. Yin, “Extracting conditional formulas for cross-platform bug search,” in Proceedings of the 2017 ACM on Asia Conference on Computer and Communications Security, AsiaCCS 2017, Abu Dhabi, United Arab Emirates, April 2-6, 2017. ACM, 2017, pp. 346–359.
- [40] S. Eschweiler, K. Yakdan, and E. Gerhards-Padilla, “discovre: Efficient cross-architecture identification of bugs in binary code,” in 23rd Annual Network and Distributed System Security Symposium, NDSS 2016, San Diego, California, USA, February 21-24, 2016. The Internet Society, 2016.
- [41] T. Dullien and R. Rolles, “Graph-based comparison of executable objects (english version),” in SSTIC, vol. 5, 2005, p. 3.
- [42] Q. Feng, R. Zhou, C. Xu, Y. Cheng, B. Testa, and H. Yin, “Scalable graph-based bug search for firmware images,” in Proceedings of the 2016 ACM SIGSAC Conference on Computer and Communications Security, Vienna, Austria, October 24-28, 2016. ACM, 2016, pp. 480–491.

- [43] N. Marastoni, R. Giacobazzi, and M. D. Preda, "A deep learning approach to program similarity," in Proceedings of the 1st International Workshop on Machine Learning and Software Engineering in Symbiosis, MASES@ASE 2018, Montpellier, France, September 3, 2018. ACM, 2018, pp. 26–35.
- [44] J. Gao, X. Yang, Y. Fu, Y. Jiang, and J. Sun, "Vulseeker: a semantic learning-based vulnerability seeker for cross-platform binary," in Proceedings of the 33rd ACM/IEEE International Conference on Automated Software Engineering, ASE 2018, Montpellier, France, September 3-7, 2018. ACM, 2018, pp. 896–899.
- [45] L. Massarelli, G. A. D. Luna, F. Petroni, L. Querzoni, and R. Baldoni, "Investigating graph embedding neural networks with unsupervised features extraction for binary analysis," in Proceedings of the Workshop on Binary Analysis Research (BAR) 2019, San Diego, CA, USA, 2019.
- [46] Y. Li, C. Gu, T. Dullien, O. Vinyals, and P. Kohli, "Graph matching networks for learning the similarity of graph structured objects," in Proceedings of the 36th International Conference on Machine Learning, ICML 2019, 9-15 June 2019, Long Beach, California, USA, ser. Proceedings of Machine Learning Research, vol. 97. PMLR, 2019, pp. 3835–3845.
- [47] S. Arakelyan, S. Arasteh, C. Hauser, E. Kline, and A. Galstyan, "Bin2vec: learning representations of binary executable programs for security tasks," *Cybersecur.*, vol. 4, no. 1, 2021.
- [48] Y. Wang, P. Jia, C. Huang, J. Liu, and P. He, "Hierarchical attention graph embedding networks for binary code similarity against compilation diversity," *Secur. Commun. Networks*, vol. 2021, pp. 9 954 520:1–9 954 520:19, 2021.
- [49] S. Yang, L. Cheng, Y. Zeng, Z. Lang, H. Zhu, and Z. Shi, "Asteria: Deep learning-based ast-encoding for cross-platform binary code similarity detection," in 51st Annual IEEE/IFIP International Conference on Dependable Systems and Networks, DSN 2021, Taipei, Taiwan, June 21-24, 2021. IEEE, 2021, pp. 224–236.
- [50] T. Mikolov, I. Sutskever, K. Chen, G. S. Corrado, and J. Dean, "Distributed representations of words and phrases and their compositionality," in Advances in Neural Information Processing Systems 26: 27th Annual Conference on Neural Information Processing Systems 2013. Proceedings of a meeting held December 5-8, 2013, Lake Tahoe, Nevada, United States, 2013, pp. 3111–3119.
- [51] Z. Luo, T. Hou, X. Zhou, H. Zeng, and Z. Lu, "Binary code similarity detection through LSTM and Siamese neural network," *EAI Endorsed Trans. Security Safety*, vol. 8, no. 29, p. e1, 2021.
- [52] H. Koo, S. Park, D. Choi, and T. Kim, "Semantic-aware binary code representation with BERT," *CoRR*, vol. abs/2106.05478, 2021.
- [53] Sunwoo Ahn, Seongwan Ahn, H. Koo, and Y. Paek, "Practical binary code similarity detection with bert-based transferable similarity learning," in Annual Computer Security Applications Conference, ACSAC 2022, Austin, TX, USA, December 5-9, 2022. ACM, 2022, pp. 361–374.
- [54] X. Zhang, W. Sun, J. Pang, F. Liu, and Z. Ma, "Similarity metric method for binary basic blocks of cross-instruction set architecture," in Proceedings of the Workshop on Binary Analysis Research (BAR) 2020, 23 February 2020, San Diego, CA, USA, 2020.
- [55] Y. Duan, X. Li, J. Wang, and H. Yin, "Deepbindiff: Learning program-wide code representations for binary diffing," in 27th Annual Network and Distributed System Security Symposium, NDSS 2020, San Diego, California, USA, February 23-26, 2020. The Internet Society, 2020.
- [56] C. Yang, Z. Liu, D. Zhao, M. Sun, and E. Y. Chang, "Network representation learning with rich text information," in Proceedings of the Twenty-Fourth International Joint Conference on Artificial Intelligence, IJCAI 2015, Buenos Aires, Argentina, July 25-31, 2015. AAAI Press, 2015, pp. 2111–2117.
- [57] N. Lageman, E. D. Kilmer, R. J. Walls, and P. D. McDaniel, "Bindnn: Resilient function matching using deep learning," in Security and Privacy in Communication Networks - 12th International Conference, SecureComm 2016,



Guangzhou, China, October 10-12, 2016, Proceedings, ser. Lecture Notes of the Institute for Computer Sciences, Social Informatics and Telecommunications Engineering, vol. 198. Springer, 2016, pp. 517–537.

- [58] L. Yu, Y. Lu, Y. Shen, H. Huang, and K. Zhu, “Bedetector: A two-channel encoding method to detect vulnerabilities based on binary similarity,” *IEEE Access*, vol. 9, pp. 51 631–51 645, 2021.
- [59] J. Yang, C. Fu, X. Liu, H. Yin, and P. Zhou, “Codee: A tensor embedding scheme for binary code search,” *IEEE Trans. Software Eng.*, vol. 48, no. 7, pp. 2224–2244, 2022.
- [60] Z. Yu, R. Cao, Q. Tang, S. Nie, J. Huang, and S. Wu, “Order matters: Semantic-aware neural networks for binary code similarity detection,” in *The Thirty-Fourth AAAI Conference on Artificial Intelligence, AAAI 2020, The Thirty-Second Innovative Applications of Artificial Intelligence Conference, IAAI 2020, The Tenth AAAI Symposium on Educational Advances in Artificial Intelligence, EAAI 2020, New York, NY, USA, February 7-12, 2020*. AAAI Press, 2020, pp. 1145–1152.
- [61] J. Gilmer, S. S. Schoenholz, P. F. Riley, O. Vinyals, and G. E. Dahl, “Neural message passing for quantum chemistry,” in *Proceedings of the 34th International Conference on Machine Learning, ICML 2017, Sydney, NSW, Australia, 6-11 August 2017*, ser. *Proceedings of Machine Learning Research*, vol. 70. PMLR, 2017, pp. 1263–1272.
- [62] J. Su, “Simbert: Integrating retrieval and generation into bert,” <https://github.com/ZhuiyiTechnology/simbert>, 2020.
- [63] L. Dong, N. Yang, W. Wang, F. Wei, X. Liu, Y. Wang, J. Gao, M. Zhou, and H.-W. Hon, “Unified language model pre-training for natural language understanding and generation,” in *Advances in Neural Information Processing Systems 32: Annual Conference on Neural Information Processing Systems 2019, NeurIPS 2019, December 8-14, 2019, Vancouver, BC, Canada, 2019*, pp. 13 042–13 054.
- [64] P. Junod, J. Rinaldini, J. Wehrli, and J. Michielin, “Obfuscator llvm software protection for the masses,” in *1st IEEE/ACM International Workshop on Software Protection, SPRO 2015, Florence, Italy, May 19, 2015*. IEEE Computer Society, 2015, pp. 3–9.
- [65] RadareOrg, “radare2,” <https://github.com/radareorg/radare2>, 2022.
- [66] SecretPatch, “Vulnerabilities dataset,” <https://github.com/SecretPatch/Dataset>, 2022.
- [67] InnerEye, “Innereye open-source code,” <https://nmt4binaries.github.io/>, 2023.
- [68] DeepBinDiff, “Deepbindiff open-source code,” <https://github.com/yueduan/DeepBinDiff>, 2023.
- [69] oalieno, “Unofficial implementation of asm2vec using pytorch,” <https://github.com/oalieno/asm2vec-pytorch>, 2022.
- [70] S. Team, “Official implementation of safe,” <https://github.com/gadiluna/SAFE>, 2022.
- [71] P. Team, “Official implementation of palmtree,” <https://github.com/palmtree/PalmTree>, 2022.
- [72] jTrans Team, “Official implementation of jtrans,” <https://github.com/vul337/jTrans>, 2022.
- [73] Hex-rays, “Ida pro disassembler and debugger,” <https://www.hex-rays.com/products/ida/index.shtml>, 2022.
- [74] R. Sennrich, B. Haddow, and A. Birch, “Neural machine translation of rare words with subword units,” in *Proceedings of the 54th Annual Meeting of the Association for Computational Linguistics, ACL 2016, August 7-12, 2016, Berlin, Germany, Volume 1: Long Papers*. The Association for Computer Linguistics, 2016.
- [75] M. Schuster and K. Nakajima, “Japanese and korean voice search,” in *2012 IEEE International Conference on Acoustics, Speech and Signal Processing, ICASSP 2012, Kyoto, Japan, March 25-30, 2012*. IEEE, 2012, pp. 5149–5152.
- [76] L. van der Maaten and G. E. Hinton, “Visualizing data using t-sne,” *Journal of Machine Learning Research*, vol. 9, pp. 2579–2605, 2008.